P345

Two-dimensional Elastic Full-waveform Inversion of Passive Teleseismic Data for Lithospheric Imaging

D. Pageot* (GeoAzur / Nice Sophia Antipolis University), S. Operto (GeoAzur / Nice Sophia Antipolis University), M. Vallée (GeoAzur / Nice Sophia Antipolis University), R. Brossier (ISTerre / Université Joseph Fourier) & J. Virieux (ISTerre / Université Joseph Fourier)

SUMMARY

We present a parametric analysis of 2D elastic frequency-domain full-waveform inversion of passive teleseismic data for lithospheric imaging. In the framework of teleseismic experiments, the sources are few compressional plane waves, which impinges the base of the lithospheric target located below the receiver arrays. To overcome the narrow aperture illumination provided by such source-receiver configuration, P and SV converted waves at the free-surface, acting as secondary sources, are crucial for increasing the illumination of the target zone. The P and S wavespeeds are jointly updated during the inversion. The resolution of the P and S wave-velocity models is dramatically improved when free-surface effects are involved in the inversion. A hierarchical inversion procedure of finely sampled frequency groups prevents spatial aliasing in depth, while the inversion is less sensitive to the sampling of the incidence angles of the plane-wave sources. The receiver interval must be lower than half the shear wavelengths in the near surface to prevent horizontal aliasing artifacts in the S-wave velocity model. A key feature of teleseismic experiments is the low frequency content of the source (0.05 - 1 Hz), which should allow one to use simple initial models without cycle skipping artifacts.

Introduction

During the last few years, full waveform inversion (FWI) has been mainly developed for controlled-source seismic exploration to build high-resolution P-wave velocity models (Virieux and Operto, 2009). Spectacular applications of 3D FWI have been shown, when the imaging takes advantage of the strong data redundancy offered by dense 3D wide-aperture seismic surveys (Sirgue et al., 2010). Multi-parameter FWI based on the elastic wave equation is the next step for recovering more realistic multi-parameter subsurface models, amenable to lithological inferences. Elastic FWI is challenging because multi-parameter inversion, which involves parameters with variable footprint in the data, can be highly nonlinear, in particular when high-amplitude surface waves in land environments are inverted (Tarantola, 1986; Brossier et al., 2009). We present an adaptation of frequency-domain elastic FWI to passive teleseismic data for lithospheric imaging. Far-distance earthquakes are considered as incident compressional plane waves, which impinge the base of the lithospheric target before their recording on the surface. In this setting, there are several key differences with conventional controlled-source acquisitions: the number of up-going plane-wave sources is generally small and leads to a narrow aperture illumination of the subsurface. For overcoming this limited illumination and for improving the resolution of the imaging, considering all reflections and conversions from the lithospheric reflectors is crucial. These conversions are generated after a first reflection from the free surface (Bostock et al., 2001), leading to a complementary reflection illumination. Compared to efficient frequency-domain FWI, where few discrete frequencies are processed sequentially (Sirgue and Pratt, 2004), the limited angular illumination provided by teleseismic experiments requires several simultaneous inversions of finely-sampled frequency groups to avoid aliasing artifacts. Moreover, receiver arrays for teleseismic experiments are significantly coarser ($> 5\ km$) than arrays deployed during controlled-source experiments and, therefore, the maximum receiver interval, which allows us to prevent horizontal aliasing in the reconstruction, should be assessed according to the propagated teleseismic wavelengths. Teleseismic experiments are also characterized by the low-frequency content of the sources, typically between 0.05 Hz and 1 Hz, which should allow one to start the inversion from simple starting models without fearing cycle skipping trapping the optimization into a secondary minimum. We address these issues by means of a parametric analysis of elastic FWI performed in a teleseismic setting. This study may provide some guidelines to view elastic FWI of passive and active data at different exploration scales.

Elastic full waveform inversion: method and resolution analysis

In this study, 2D elastic FWI is performed in the frequency domain using a discontinuous Galerkin modeling engine on unstructured triangular meshes (Brossier, 2011). The P- and S-wave speeds (V_p and V_s, respectively) are jointly updated during the inversion of the vertical and horizontal geophone data. Optimization relies on a conjugate-gradient algorithm, where the gradient of the L_2 misfit function is computed with the adjoint-state method. Multiscale FWI is implemented by successive inversions of frequency groups of increasing high-frequency content. Incident compressional plane-wave sources are implemented with a scattered-field formulation (Pageot et al., 2010; Roecker et al., 2010), and a free-surface boundary condition is used on the top of the mesh. The free-surface reflects downward P and SV plane waves, which are used as secondary sources to perform surface reflection tomography. Worth of note, no surface waves are generated in a homogeneous half-space for up-going compressional plane waves. Therefore, the footprint of surface waves in our elastic FWI should be quite small.

A resolution analysis of FWI allows one to relate the local wavenumber $\mathbf{k}$ reconstructed at a diffractor point to the frequency f and the aperture angle θ as

$$\mathbf{k} = \frac{2f}{c_0} cos\,(\theta/2)\,\mathbf{n}, \tag{1}$$

where the background velocity is denoted by c_0 and a unit vector in the direction of $\mathbf{k}$ by $\mathbf{n}$ (Fig. 1a) (*e.g.*, Sirgue and Pratt, 2004). This relationship shows the redundant control of frequency and aperture angle on the wavenumber coverage. When dense wide-aperture data are considered, Pratt (1999)

has proposed to decimate the redundancy of the wavenumber coverage by limiting the inversion to few discrete frequencies. A criterion for selecting frequency, which leads to an increasing frequency interval as the inversion proceeds towards high frequency, has been proposed by Sirgue and Pratt (2004): $k_{max}(f+\Delta f) = k_{min}(f)$ (Fig. 1b) . This criterion implicitly assumes a continuous aperture sampling within the wavenumber band imaged by one frequency. This conditions is not necessarily fulfilled in teleseismic configuration, where only few sources can span over a broad band of incidence angles. In this case, inversion of finely-sampled frequency groups rather than single frequencies may be necessary to properly sample the wavenumber spectrum (Fig. 1b). A second possible scenario involves earthquakes with close incidence angles. In this case, finely-sampled frequencies are necessary to satisfy the wavenumber coverage criterion of Sirgue and Pratt (2004) (Fig. 1c). Teleseismic experiment are performed with coarse receiver arrays, while reflections of up-going plane wave sources from the free surface can be seen as a continuous line of downward mono-directional P and SV sources. For surface controlled source experiments, Brenders and Pratt (2007) show that the condition to prevent aliasing of the subsurface is such that the receiver spacing ΔR must be lower or equal to the sampling interval required to represent the horizontal features of the subsurface: $\Delta R \leq \lambda_h/2$, where λ_h denotes the horizontal wavelength.

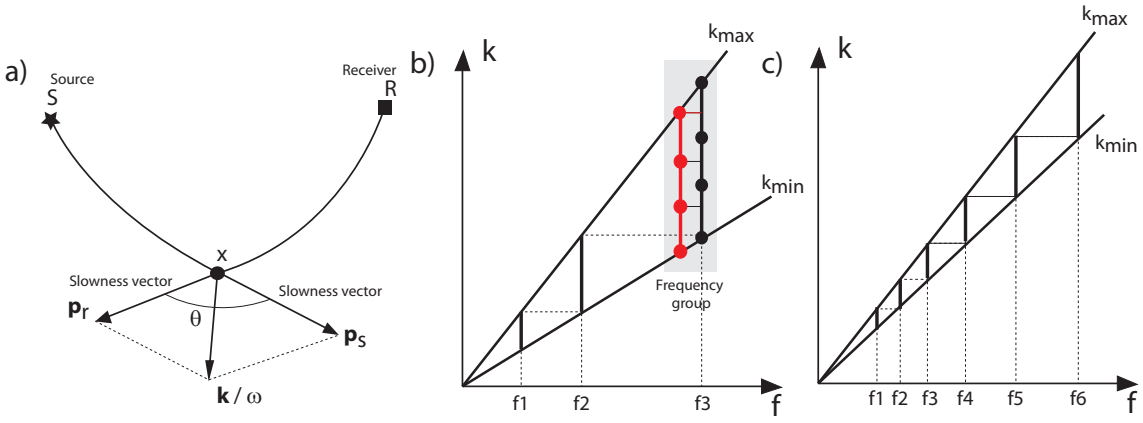

Figure 1 *(a) Relationship between local wavenumber vector* **k** *at a diffractor point, angular frequency* ω *and aperture angle* θ*. (b) Illustration of the continuous wavenumber coverage provided by few discrete frequencies (adapted from Sirgue and Pratt (2004)). The circles represents wavenumbers, which are coarsely sampled within the band spanned by one frequency in the case of teleseismic experiment. Simultaneous inversions of close multiple frequencies help to prevent undersampling of the wavenumber band (red circles). (c) Case of narrow bandwidth of incidence angles. Small frequency interval is required to guarantee the continuous sampling of the wavenumber spectrum.*

Parametric analysis of elastic FWI in teleseismic setting

We consider a synthetic case study, that corresponds to a 2D section of the SEG/EAGE overthrust model which has been scaled to lithospheric dimensions (Fig. 2a). The scaled overthrust model is 475 km x 110 km, and V_p ranges between 4500 m/s and 8000 m/s. The V_s model has been inferred from the V_p model, considering a uniform Poisson ratio of 0.25. For this parametric analysis, we consider a variable number of frequencies, which are evenly sampled within the $[0.1-0.4]$ Hz frequency band, a variable number of compressional plane-wave sources, with incidence angles evenly sampled between -40^0 and 40^0 degrees, and a line of receivers on the surface with variable receiver spacing. The multi-resolution imaging consists of successive inversions of three frequency groups: $[0.1;0.2]$ Hz, $[0.2;0.3]$ Hz and $[0.3;0.4]$ Hz. The initial models for FWI are built by smoothing the true velocity models (Fig. 2b).

We first assess the resolution improvement, which is achieved when free-surface effects are taken into account in the inversion (Fig. 3a). The final V_p and V_s FWI models, that are obtained with and without free-surface effects in the inverted data, are shown in Fig. 3(a-b). The resolution improvement achieved

when free-surface effects are taken into account in the inversions is significant for both the V_p and V_s models, and show the robustness of the elastic inversion to handle doubly-scattered events when an accurate representation of the free surface is available. It is worth noting that the free surface is not only important to increase the short-aperture illumination but also to generate S-wave sources by means of P-SV conversion at the free surface. A second key parameter is the frequency sampling. We compare the FWI results obtained with 7 and 37 frequencies in Fig. 3(b-c). The V_p model is marginally impacted by the undersampling of the frequencies, unlike the shorter-wavelength V_s model which shows a much noisier reconstruction when 7 frequencies are used. This noise is likely due to depth aliasing resulting from the undersampling of the vertical S wavenumbers. The elastic FWI is less sensitive to the incidence-angle sampling as shown by the FWI results obtained when 5 sources are used instead of 17 during inversions (Fig. 3(b, d)). This is expected because wavenumbers are linearly related to frequency, while they are related to the aperture angle by a more slowly-varying cosine function (eq. 1). The FWI models, which are obtained when the receiver spacing is 1200 m and 9600 m respectively, are shown in Fig. 3(b, e). Increasing the receiver spacing leads to horizontal aliasing artifacts in the upper part of the medium, which appear with a period corresponding to the receiver interval. Aliasing artifacts start appearing for a receiver spacing of 5 km (not shown here), which roughly corresponds to half the S-wavelength in the near surface for a 0.4 Hz frequency. This is consistent with the conclusions of Brenders and Pratt (2007). We also perform FWI for a starting frequency as low as 0.05 Hz. This frequency is within the lower limit of the source bandwidth of earthquakes of sufficiently-high magnitude and can be recorded by broadband seismometers. With such low frequencies, the quality of the V_s model has been further improved. Reliable V_p and V_s models can also be obtained using a velocity gradient model as initial model for FWI (not shown here).

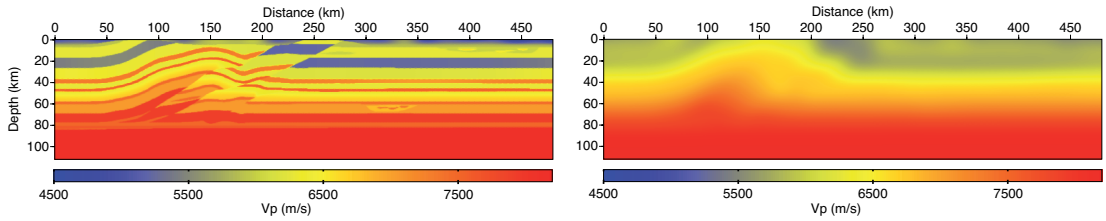

Figure 2 *(a) True and (b) initial EAGE/SEG overthrust V_p models after lithospheric scaling.*

Conclusions

The feasibility of elastic FWI of teleseismic passive data may lead to highly resolved lithospheric imaging, where sources are few up-going compressional plane waves recorded by a network of sensors on the surface as long as we are able to consider the source variability of earthquakes. We have shown the improvement in resolution, that is achieved when free-surface multiples are involved in the inversion. Removing aliasing associated with the narrow aperture illumination requires the increase of the number of frequencies involved in the inversion when compared to those needed for conventional application of efficient frequency-domain FWI. Moreover, the frequencies must be gathered into finely-sampled frequency groups. Coarse receiver spacing can lead to spatial aliasing in the near surface of the V_s model, if the receiver interval exceeds half the shear wavelengths of the near surface. The FWI might be further improved by using a second level of data preconditioning with time dampings, which will inject progressively in the inversion later-arriving phases associated with short-aperture reflections. Future work aims to apply elastic FWI to real data from the MASE experiment for the study of the Mexican subduction zone.

Acknowledgments

HPC facilities of MESOCENTRE SIGAMM computer center are gratefully acknowledged as well as the support of the staff. Partial support from grant (CINES 2280) is also acknowledged. Finally, this work was carried out within the frame of the SEISCOPE consortium (*http://seiscope.oca.eu*) sponsored by BP, CGG-Veritas, ENI,

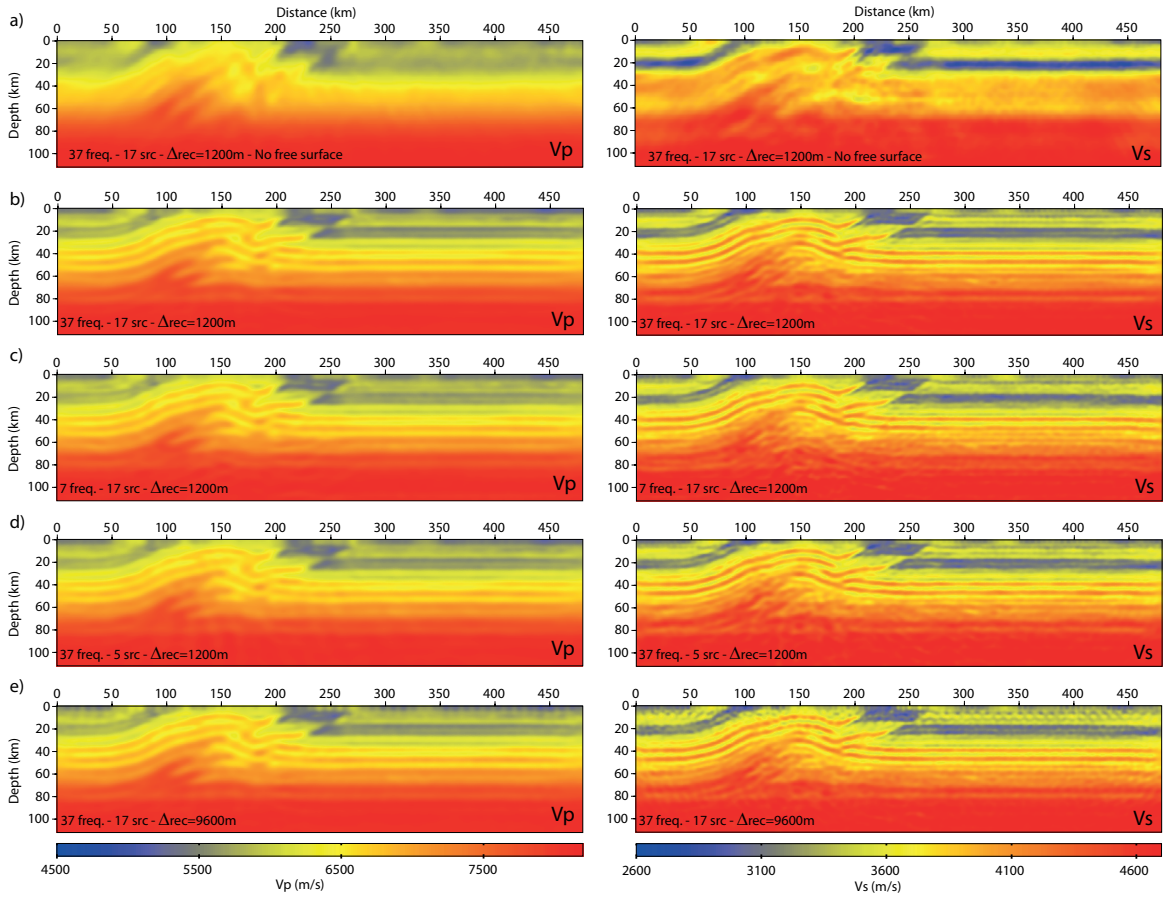

Figure 3 *(a,b) Final V_p (left) and V_s (right) FWI models for 37 frequencies (3 groups, frequency band: $[0.1 - 0.4]$ Hz) and 17 plane-wave sources (incidence angles between $\pm 40^0$ degrees). Recorded and modeled data are computed without free surface. (b) Same as (a) but free-surface effects are involved in inversion. (c) Same as (b) but 7 frequencies are inverted instead of 37. (d) Same as (b) but 5 plane-wave sources are used instead of 17. (e) Same as (b) but receiver spacing is* 9.6 *km instead of* 1.2 *km.*

EXXON-Mobil, PETROBRAS, SAUDI ARAMCO, SHELL, STATOIL and TOTAL.

References

Bostock, M.G., Rondenay, S. and Shragge, J. [2001] Multiparameter two-dimensional inversion of scattered teleseismic body waves 1. theory for oblique incidence. *Journal of Geophysical Research*, **106**(12), 30771–30782.

Brenders, A.J. and Pratt, R.G. [2007] Efficient waveform tomography for lithospheric imaging: implications for realistic 2D acquisition geometries and low frequency data. *Geophysical Journal International*, **168**, 152–170.

Brossier, R. [2011] Two-dimensional frequency-domain visco-elastic full waveform inversion: Parallel algorithms, optimization and performance. *Computers & Geosciences*, **37**(4), 444 – 455, ISSN 0098-3004, doi:DOI: 10.1016/j.cageo.2010.09.013.

Brossier, R., Operto, S. and Virieux, J. [2009] Seismic imaging of complex onshore structures by 2D elastic frequency-domain full-waveform inversion. *Geophysics*, **74**(6), WCC63–WCC76, doi:10.1190/1.3215771.

Pageot, D., Operto, S., Vallée, M., Brossie, R. and Virieux, J. [2010] Lithospheric imaging from teleseismic data by frequency-domain elastic full-waveform tomography. *Expanded abstracts*, EAGE.

Pratt, R.G. [1999] Seismic waveform inversion in the frequency domain, part I : theory and verification in a physic scale model. *Geophysics*, **64**, 888–901.

Roecker, S., Baker, B. and McLaughlin, J. [2010] A finite-difference algorithm for full waveform teleseismic tomography. *Geophysical Journal International*, **181**, 1017–1040.

Sirgue, L., Barkved, O.I., Dellinger, J., Etgen, J., Albertin, U. and Kommedal, J.H. [2010] Full waveform inversion: the next leap forward in imaging at Valhall. *First Break*, **28**, 65–70.

Sirgue, L. and Pratt, R.G. [2004] Efficient waveform inversion and imaging : a strategy for selecting temporal frequencies. *Geophysics*, **69**(1), 231–248.

Tarantola, A. [1986] A strategy for non linear inversion of seismic reflection data. *Geophysics*, **51**(10), 1893–1903.

Virieux, J. and Operto, S. [2009] An overview of full waveform inversion in exploration geophysics. *Geophysics*, **74(6)**(6), WCC127–WCC152.